

Supporting Information

Cobalt-doped δ -MnO₂ composites with CNTs as conductive framework enhance the cycling capability of aqueous zinc-ion battery

ShuLing Liu*, Jie Wang, ZiXiang Zhou, Ying Li, Wei Zhang, Chao Wang

Department of Chemistry and Chemical Engineering, Shaanxi Collaborative Innovation Center of Industrial Auxiliary Chemistry & Technology, Key Laboratory of Auxiliary Chemistry and Technology for Chemical Industry, Ministry of Education, The Youth Innovation Team of Shaanxi Universities, Shaanxi University of Science and Technology, Xi'an, Shaanxi 710021, P. R. China

*Corresponding author.

E-mail address: liushuling@sust.edu.cn

Preparation of acidified multi-walled carbon nanotubes (CNTs)

Put MWCNTs in the mixed acid of V (H₂SO₄): V (HNO₃) = 3:1 and mix well, stir at room temperature for 30 minutes, then pour the mixed solution into a three-necked flask, keep the water bath at a constant temperature of 80°C, and keep 8h reflux. After the reaction is finished, cool to room temperature, then pour the solution into a beaker and dilute it with deionized water, and make it neutral, filter and wash it with deionized water, wash it several times until it is neutral, and place the product in an oven at 60°C under vacuum dry. Finally, acidified MWCNTs were obtained.

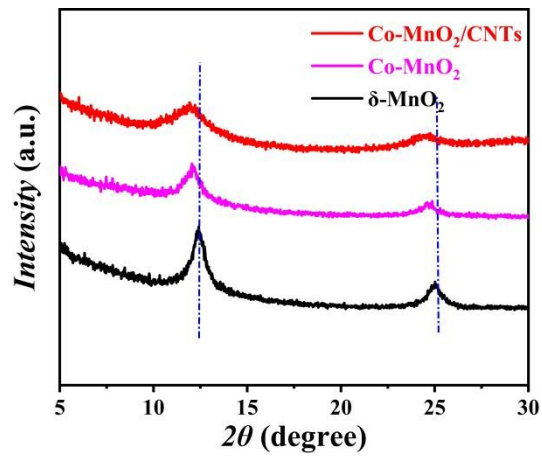


Fig. S1 Partial XRD patterns of δ -MnO₂, Co-MnO₂ and Co-MnO₂/CNTs.

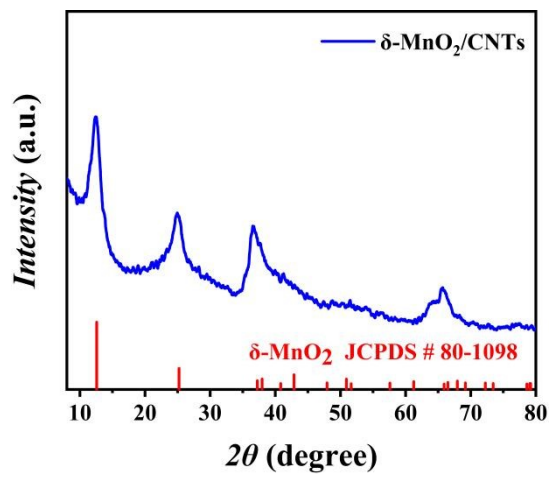


Fig. S2 XRD patterns of δ -MnO₂/CNTs.

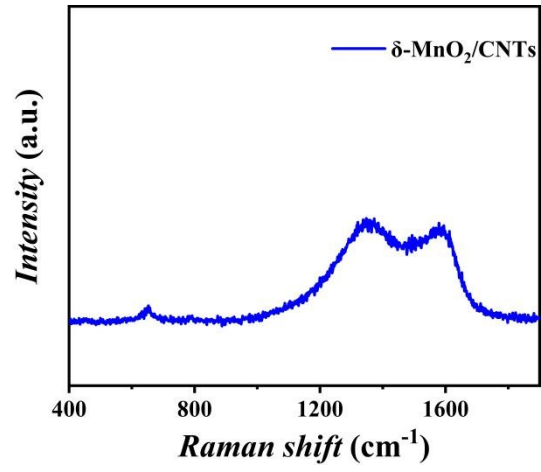


Fig. S3 Raman spectra of $\delta\text{-MnO}_2/\text{CNTs}$.

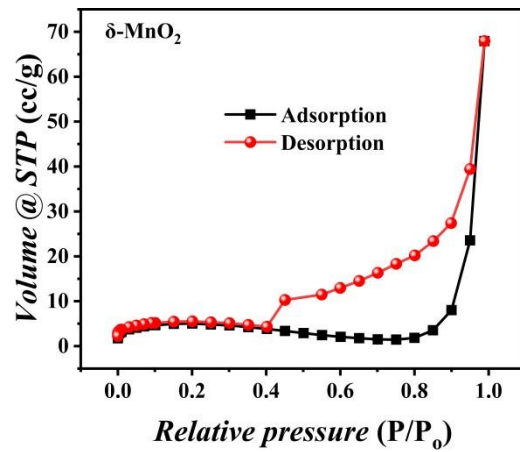


Fig. S4 N₂ adsorption–desorption isotherm of the δ -MnO₂ material.

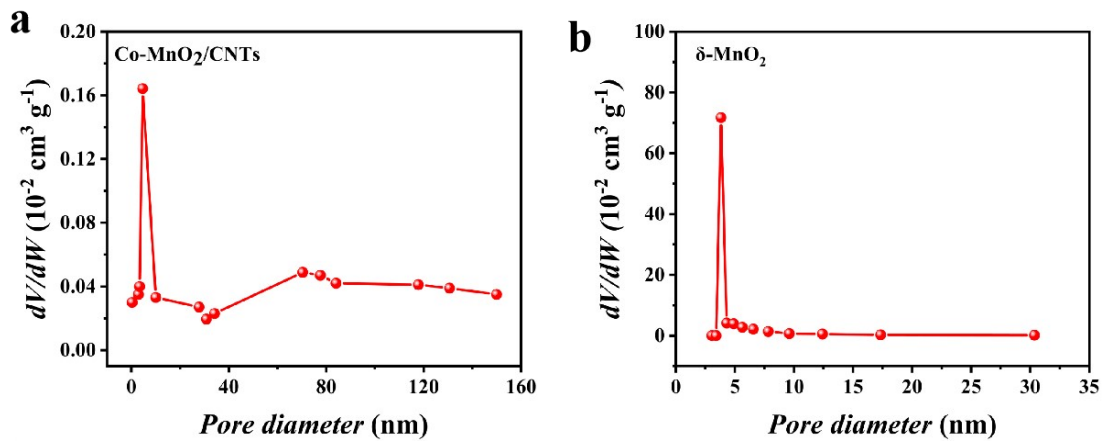


Fig. S5 Pore size distribution curve of the δ -MnO₂ and Co-MnO₂/CNTs material.

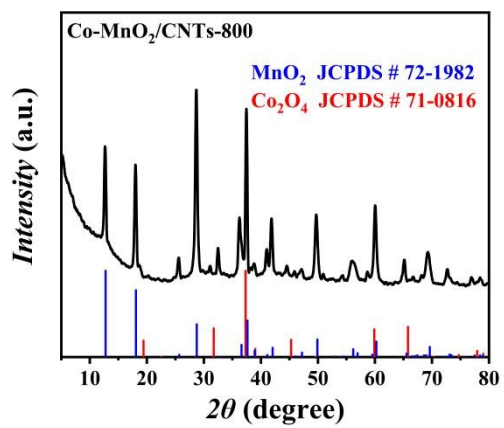


Fig. S6 Co-MnO₂/CNTs heated to 800° under air.

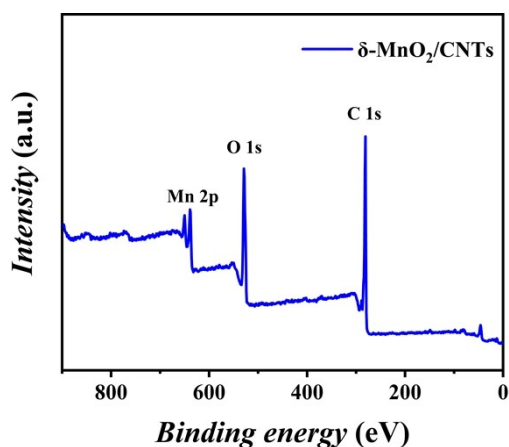


Fig. S7 XPS survey spectra (c) of $\delta\text{-MnO}_2/\text{CNTs}$.

The average oxidation state AOS of Mn in the $\text{Co-MnO}_2/\text{CNTs}$ is determined by analyzing the Mn 3s multiplet splitting magnitude (ΔE) according to the equation as follows[1]:

$$\text{AOS} = 8.95 - 1.13 \Delta E_s \text{ (eV)} \quad (\text{S1})$$

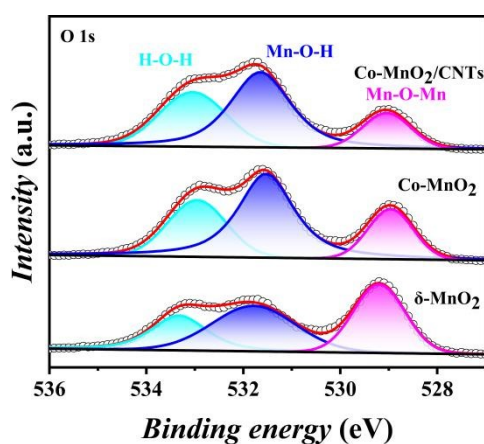


Fig. S8 O 1s spectra of $\delta\text{-MnO}_2$, Co-MnO_2 and $\text{Co-MnO}_2/\text{CNTs}$.

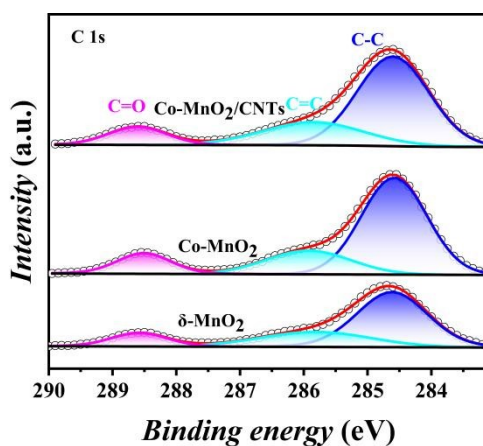


Fig. S9 C 1s spectra of $\delta\text{-MnO}_2$, Co-MnO_2 and $\text{Co-MnO}_2/\text{CNTs}$.

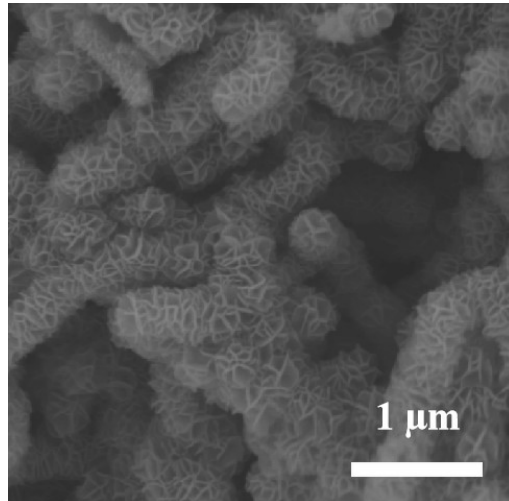


Fig. S10 SEM images of δ -MnO₂/CNTs.

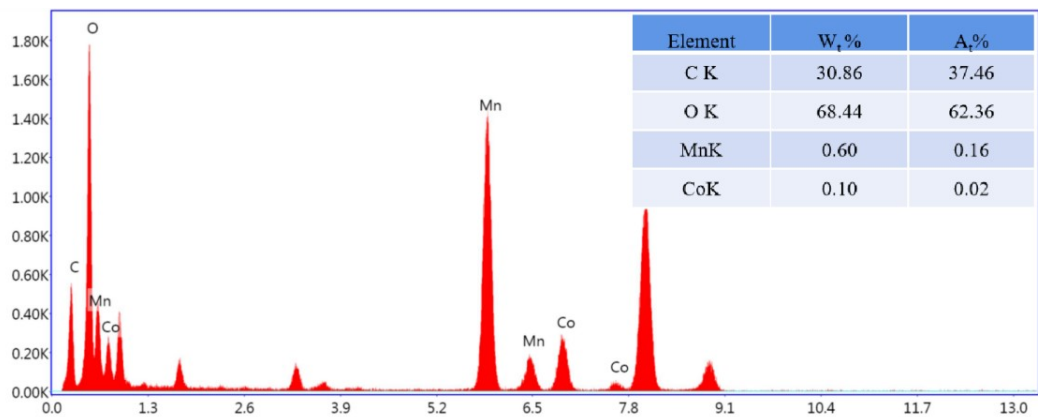


Fig. S11 EDX of the Co-MnO₂/CNTs and the corresponding elemental content (the inset).

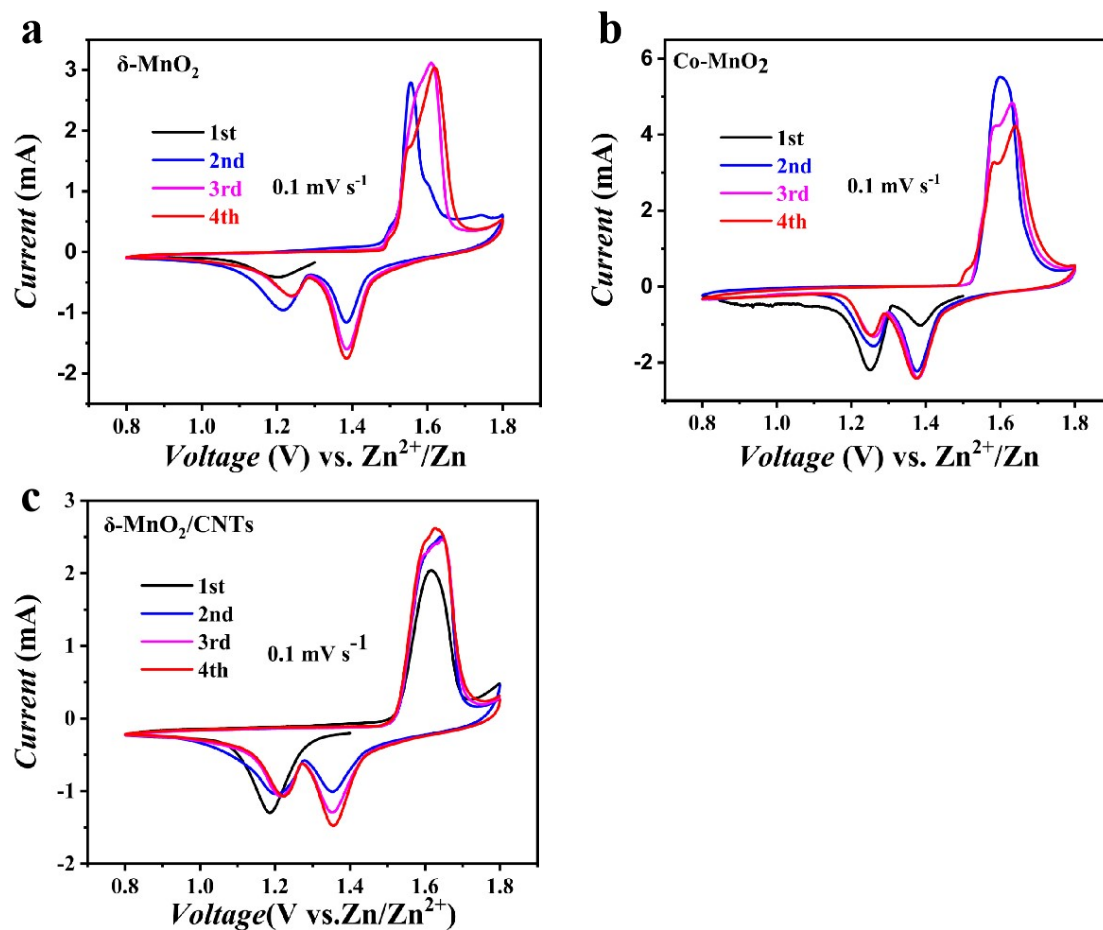


Fig. S12 CV curves of $\delta\text{-MnO}_2$, Co-MnO_2 and $\delta\text{-MnO}_2/\text{CNTs}$ at 0.1 mV s^{-1} .

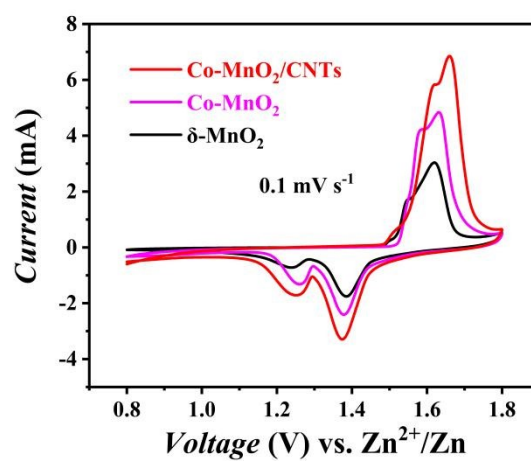


Fig. S13 CV curves of $\delta\text{-MnO}_2$, Co-MnO_2 and $\text{Co-MnO}_2/\text{CNTs}$ at 0.1 mV s^{-1} .

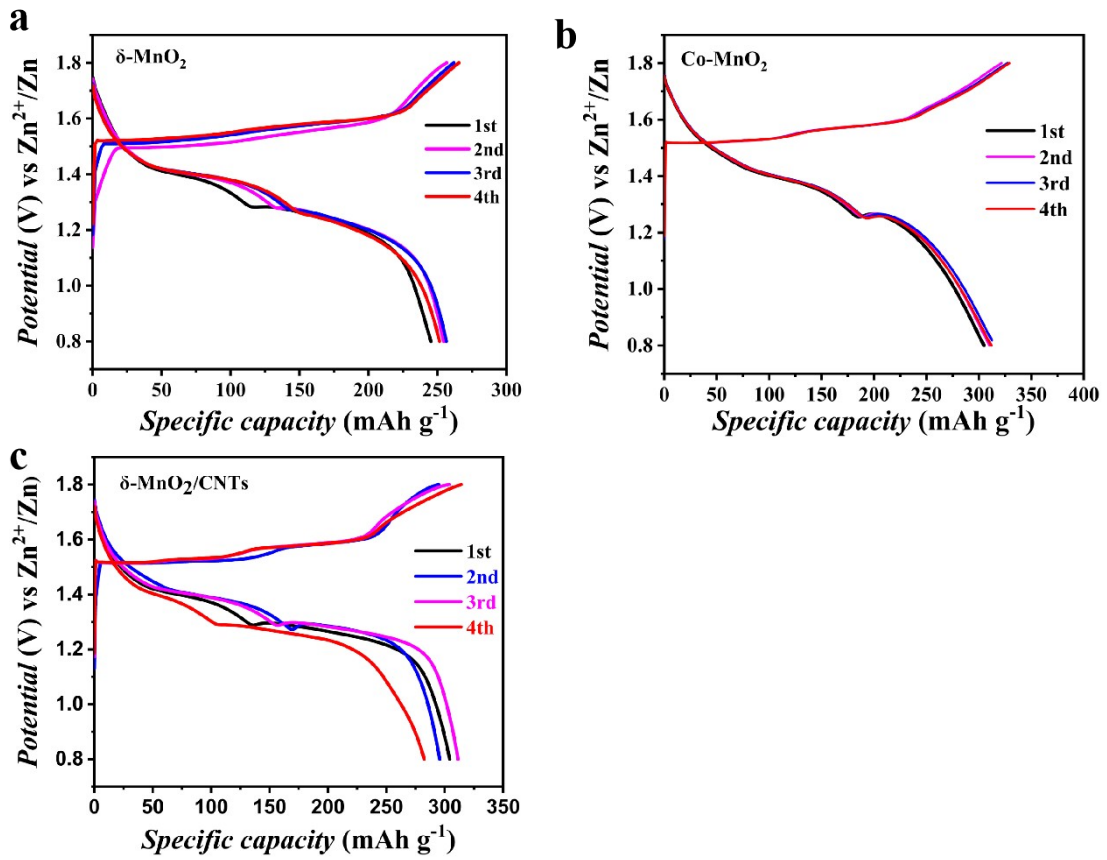


Fig. S14 GCD profiles of the $\delta\text{-MnO}_2$, Co-MnO_2 and $\delta\text{-MnO}_2/\text{CNTs}$ electrode obtained at 0.2 A g^{-1} .

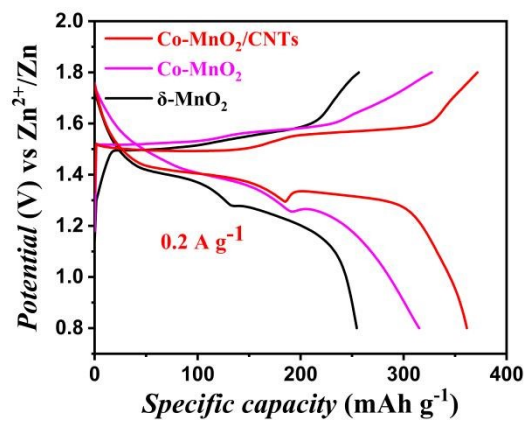


Fig. S15 Comparison of GCD profiles between $\delta\text{-MnO}_2$, Co-MnO_2 and $\text{Co-MnO}_2/\text{CNTs}$ at 0.2 A g^{-1} .

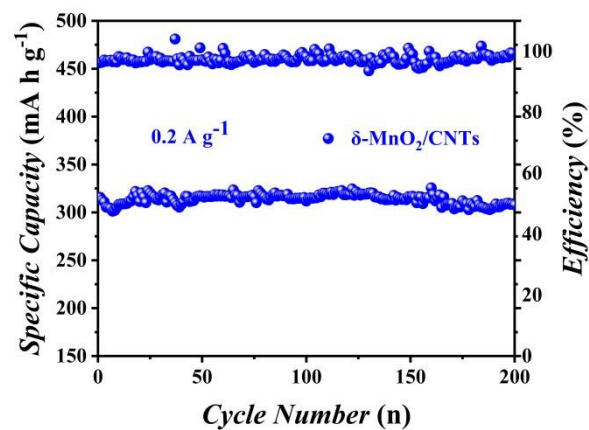


Fig. S16 Cycling performance at 0.2 A g^{-1} of the ZIBs with $\delta\text{-MnO}_2/\text{CNTs}$

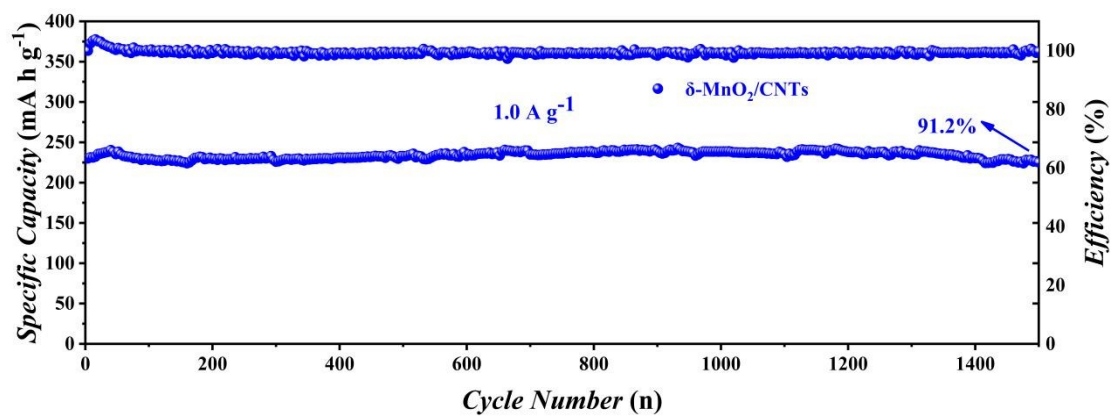


Fig. S17 Long-term cycling performance at 1.0 A g^{-1} of the ZIBs with $\delta\text{-MnO}_2/\text{CNTs}$

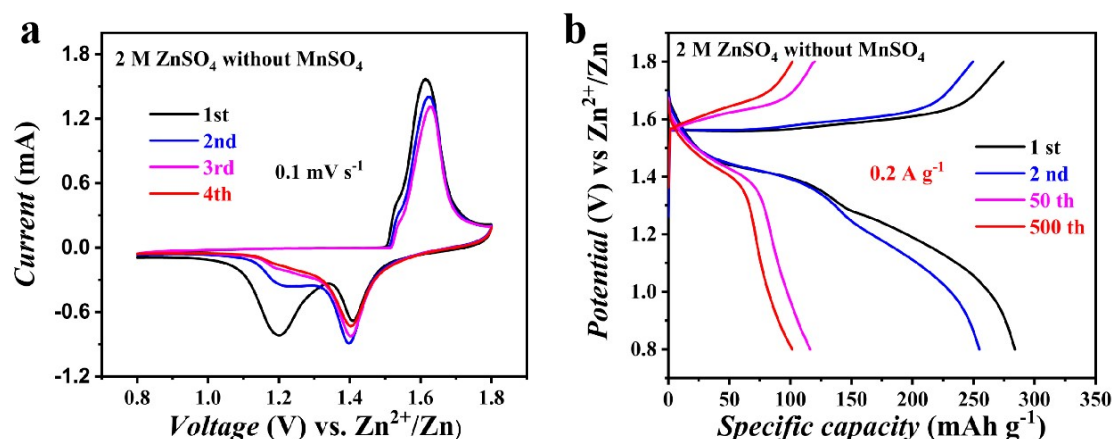


Fig. S18 a) CV curve of Co-MnO₂/CNTs battery in aqueous electrolyte (2 M ZnSO₄) at a scan of 1 mV s⁻¹. b) GCD profiles of the Co-MnO₂/CNTs electrode obtained in aqueous electrolyte (2 M ZnSO₄) at a scan of 0.2 A g⁻¹.

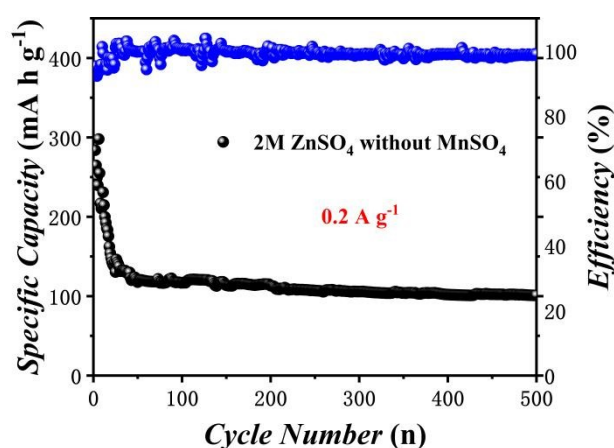


Fig. S19 Cycling performance of Co-MnO₂/CNTs at 0.2 A g⁻¹ in aqueous electrolyte (2 M ZnSO₄).

It can be found in Fig. S12a that when the electrolyte is 2 M ZnSO₄ solution, four cycles are performed at a scan rate of 0.1 mV s⁻¹, and a very clear redox peak can be observed in the first cycle under the premise of an open circuit voltage of 1.63 V, but the reduction peak at around 1.2 V gradually disappeared as the number of cycles increased. Corresponding to the GCD curve in Fig. S12b at 0.2 mA g⁻¹, the discharge curve platform located in the 1.2-1.3 V was also gradually disappeared. To this end, the battery was tested for 500 cycles at 0.2 mA g⁻¹. It was found that the capacity of the Co-MnO₂/CNTs sample gradually decreased from 283 mAh g⁻¹ to 101 mAh g⁻¹ when without Mn²⁺ was added to the electrolyte, the capacity retention rate is only 35.6%.

Table S1. Performance comparison of aqueous ZIBs with manganese oxide-based materials as cathodes.

Cathode material	Electrolyte	Specific capacity	Capacity retention	Ref.
Co-MnO ₂ /CNTs	2 M ZnSO ₄ + 0.2 M MnSO ₄	365 mA h g ⁻¹ at 0.2 A g ⁻¹	94.6% after 1500 cycles at 1 A g ⁻¹	This work
α-MnO ₂	1 M ZnSO ₄	233 mA h g ⁻¹ at 0.083 A g ⁻¹	63% after 50 cycles at 0.083 A g ⁻¹	[2]
β-MnO ₂	1 M ZnSO ₄	247 mA h g ⁻¹ at 0.066 A g ⁻¹	75% after 200 cycles at 0.2 A g ⁻¹	[3]
δ-MnO ₂	1 M ZnSO ₄	252 mA h g ⁻¹ at 0.083 A g ⁻¹	43% after 100 cycles at 0.083 A g ⁻¹	[4]
Bi-α-MnO ₂	2 M ZnSO ₄ + 0.2 M MnSO ₄	325 mA h g ⁻¹ at 0.3 A g ⁻¹	90.9% after 2000 cycles at 1 A g ⁻¹	[5]
ZnMn ₂ O ₄ /NG	1 M ZnSO ₄ + 0.05 M MnSO ₄	232 mA h g ⁻¹ at 0.1 A g ⁻¹	97.4% after 2500 cycles at 1 A g ⁻¹	[6]
Mn ₂ O ₃ @PPy	2 M ZnSO ₄ + 0.1 M MnSO ₄	255 mA h g ⁻¹ at 0.1 A g ⁻¹	No decreasing after 2000 cycles at 0.4 A g ⁻¹	[7]
δ-NMOH	2 M ZnSO ₄ + 0.2 M MnSO ₄	232 mA h g ⁻¹ at 2 C	Nearly 100% after 2000 cycles at 10 C	[8]
Mn ₃ O ₄	2 M ZnSO ₄	232 mA h g ⁻¹ at 0.2 A g ⁻¹	No decreasing after 300 cycles at 0.5 A g ⁻¹	[9]
Zn-δ-MnO ₂	2 M ZnSO ₄ + 0.2 M MnSO ₄	278 mA h g ⁻¹ at 0.38 A g ⁻¹	98% after 10000 cycles at 7 A g ⁻¹	[10]

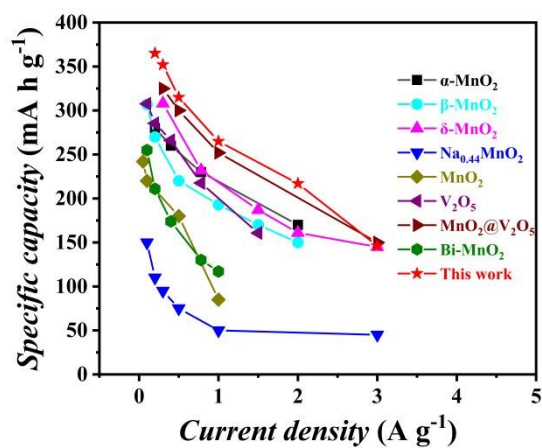


Fig. S20 Compared with other ZIBs Mn-based electrodes previously reported, the specific capacity (stable capacity) of Co-MnO₂/CNTs is higher at different current densities.

Table S2. The R_s and R_{ct} values of pristine Co-MnO₂/CNTs, Co-MnO₂ and δ -MnO₂ cathodes.

Samples	R_s /Ohm	R_{ct} /Ohm
Co-MnO ₂ /CNTs	3.474	28.33
Co-MnO ₂	3.983	67.68
δ -MnO ₂	6.904	91.33

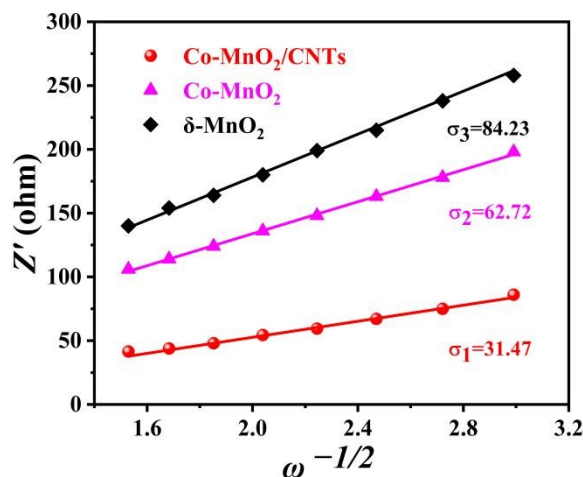


Fig. S21 Relationship between Z' and $\omega^{-1/2}$ of the electrodes in the low frequency region.

According to the reported literatures, the ion diffusion coefficient (D) could be calculated via the following equations[11]:

$$Z' = R_s + R_f + R_{ct} + \sigma \omega^{-1/2} \quad (S2)$$

$$D = \frac{0.5R^2T^2}{A^2\sigma^2C^2n^4F^4}$$

(S3)

where R is the gas constant, T is the absolute temperature, A is the contact area of the electrode with electrolyte, n is the number of electrons per formula during oxidation, F is the Faraday constant, C is the concentration of zinc ions and σ is the Warburg factor, which is equaled to the slope of $Z' - \omega^{-1/2}$. Z' and ω are imaginary resistance and angular speed, respectively.

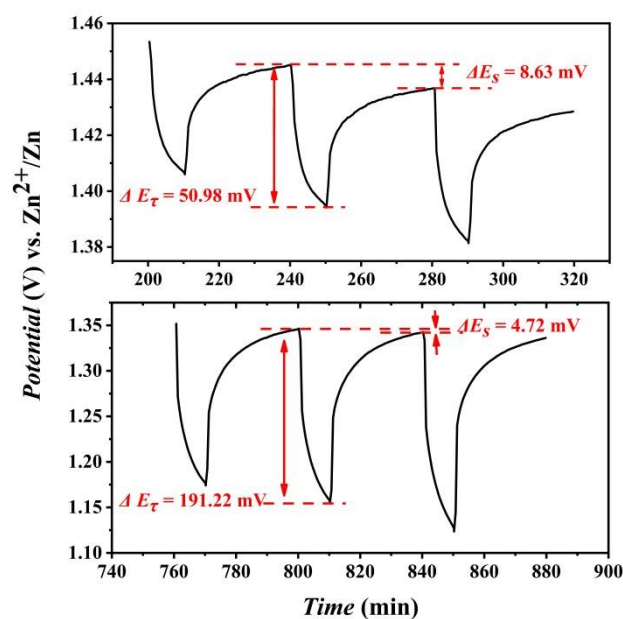


Fig. S22 Enlarged parts of the GITT curves at the two platforms of the discharge process.

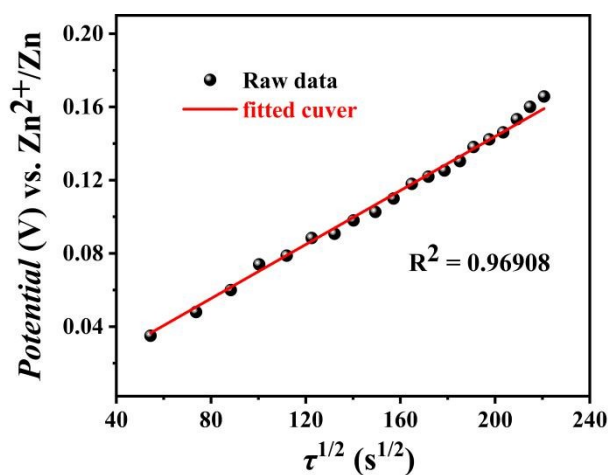


Fig. S23 Linear relationship of ΔE_{τ} and $\tau^{1/2}$ at the discharge process.

The GITT measurement of Co-MnO₂/CNTs electrode was conducted at the current density of 0.1 A g⁻¹. The charging time and rest time are 10 min and 30 min, respectively. As shown in Fig. S16, the voltage (ΔE_{τ}) exhibits a linear behavior with the square root of the titration time ($\tau^{1/2}$)[12]. Therefore, the diffusion coefficient can be calculated based on the Equation (S3):

$$D = \frac{4}{\pi} \left(\frac{m_B V_M}{M_B A} \right)^2 \left(\frac{\Delta E_S}{\Delta E_\tau} \right)^2 \quad (\text{S4})$$

Here, τ is the constant pulse time 30 min, m_B is the mass of the active material, V_M is the molar volume, m_B is the molecular weight, A is the surface area of electrode with electrode, and ΔE_τ is the difference of stabilized open-circuit for the corresponding step[13]. Accordingly, in this Co-MnO₂/CNTs battery, the relationship between diffusion coefficient and $(\Delta E_s/\Delta E_\tau)^2$ can be described as Eq. S4:

$$\frac{D_1}{D_2} = \frac{\left(\frac{\Delta E_{S,1}}{\Delta E_{\tau,1}} \right)^2}{\left(\frac{\Delta E_{S,2}}{\Delta E_{\tau,2}} \right)^2} \quad (\text{S5})$$

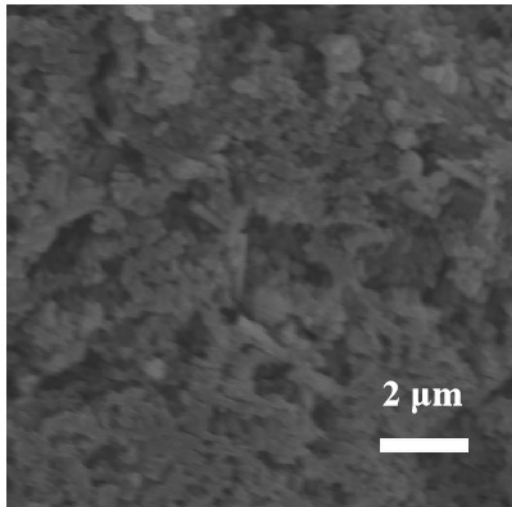


Fig. S24 SEM of the Co-MnO₂/CNTs electrode after 10 cycles.

Supplementary References

- [1] Y. Yang, Y. Li, M. Zeng, M. Mao, L. Lan, H. Liu, J. Chen and X. Zhao, UV-vis-infrared light-driven photothermocatalytic abatement of CO on Cu doped ramsdellite MnO₂ nanosheets enhanced by a photoactivation effect, *Applied Catalysis B Environmental*, 2018, **224**, 751-760.
- [2] B. Wu, G. Zhang, M. Yan, T. Xiong, P. He, L. He, X. Xu and L. Mai, Graphene Scroll-Coated α -MnO₂ Nanowires as High-Performance Cathode Materials for Aqueous Zn-Ion Battery, *Small*, 2018, **14**.
- [3] S. Islam, M. H. Alfaruqi, V. Mathew, J. Song, S. Kim, S. Kim, J. Jo, J. P. Baboo, D. T. Pham and D. Y. Putro, Facile synthesis and the exploration of the zinc storage mechanism of β -MnO₂ nanorods with exposed (101) planes as a novel cathode material for high performance eco-friendly zinc-ion batteries, *Journal of Materials Chemistry A*, 2017, **5**, 23299-23309.
- [4] M. H. Alfaruqi, J. Gim, S. Kim, J. Song, D. T. Pham, J. Jo, Z. Xiu, V. Mathew and J. Kim, A layered δ -MnO₂ nanoflake cathode with high zinc-storage capacities for eco-friendly battery applications, *Electrochemistry Communications*, 2015.
- [5] K. Ma, Q. Li, C. Hong, G. Yang and C. Wang, Bi Doping-Enhanced Reversible-Phase Transition of α -MnO₂ Raising the Cycle Capability of Aqueous Zn-Mn Batteries, *ACS Applied Materials & Interfaces*, 2021, **13**, 55208-55217.
- [6] L. Chen, Z. Yang, H. Qin, X. Zeng and J. Meng, Advanced electrochemical performance of ZnMn₂O₄/N-doped graphene hybrid as cathode material for zinc ion battery, *Journal of Power Sources*, 2019, **425**, 162-169.
- [7] N. Liu, X. Wu, Y. Yin, A. Chen, C. Zhao, Z. Guo, L. Fan and N. Zhang, Constructing the efficient ion diffusion pathway by introducing oxygen defects in Mn₂O₃ for high-performance aqueous zinc-ion batteries, *ACS applied materials & interfaces*, 2020, **12**, 28199-28205.

- [8] D. Wang, L. Wang, G. Liang, H. Li, Z. Liu, Z. Tang, J. Liang and C. Zhi, A superior δ -MnO₂ cathode and a self-healing Zn- δ -MnO₂ battery, *ACS nano*, 2019, **13**, 10643-10652.
- [9] J. Hao, J. Mou, J. Zhang, L. Dong, W. Liu, C. Xu and F. Kang, Electrochemically induced spinel-layered phase transition of Mn₃O₄ in high performance neutral aqueous rechargeable zinc battery, *Electrochimica Acta*, 2018, **259**, 170-178.
- [10] D. Wang, L. Wang, G. Liang, H. Li and C. Zhi, A Superior δ -MnO₂ Cathode and a Self-Healing Zn- δ -MnO₂ Battery, *ACS Nano*, 2019, **13**.
- [11] K. W. Knehr, S. Biswas and D. A. Steingart, Quantification of the Voltage Losses in the Minimal Architecture Zinc-Bromine Battery Using GITT and EIS, *Journal of the Electrochemical Society*, 2017, **164**, A3101-A3108.
- [12] C. Heubner, M. Schneider and A. Michaelis, SoC dependent kinetic parameters of insertion electrodes from staircase — GITT, *Journal of electroanalytical chemistry*, 2016, **767**, 18-23.
- [13] E. Deiss, Spurious chemical diffusion coefficients of Li⁺ in electrode materials evaluated with GITT, *Electrochimica Acta*, 2005, **50**, 2927-2932.